Solar Energy Materials & Solar Cells 93 (2009) 1881–1884

Contents lists available at ScienceDirect

Solar Energy Materials & Solar Cells

journal homepage: www.elsevier.com/locate/solmat

Study of silicon solar cell at different intensities of illumination and wavelengths using impedance spectroscopy

Sanjai Kumar [a], P.K. Singh [a,*], G.S. Chilana [b]

[a] National Physical Laboratory, K.S. Krishnan Road, New Delhi-110012, India
[b] Ramjas College, University of Delhi, Delhi-110007, India

ARTICLE INFO

Article history:
Received 17 January 2009
Received in revised form
23 June 2009
Accepted 1 July 2009
Available online 25 July 2009

Keywords:
Solar cell
Impedance spectroscopy
Dynamic and static characteristics
Spectral response

ABSTRACT

The electrical properties of an n^+–p–p^+ structure-based single-crystalline silicon solar cell were studied by impedance spectroscopy, *I–V* and spectral response. The impedance spectrum is measured in dark, under different intensities (14, 43, 57, 71, 86, 100 mW/cm^2) of illumination and wavelengths (400–1050 nm) of light. Under dark and at low intensities of illumination (<50 mW/cm^2) the impedance spectra show perfect semicircles but at high intensities the semicircles are distorted at low frequencies. It is found that illumination provides an additional virtual R_1C_1 network parallel to the initial bulk R_pC_p network observed under dark conditions. The value of virtual resistance R_1 depends on the illumination wavelength and shows an inverse relationship with the spectral response of the device.

1. Introduction

Impedance spectroscopy (IS) [1] is a non-destructive technique, which is sensitive to small changes in the system and is generally employed by electrochemists to study characteristics of batteries, electrodes and corrosion-related problems. This technique is widely applied to systems modelled by an equivalent circuit to determine their dynamic (ac) characteristics from which physical parameters of the system can be calculated. Impedance spectroscopy is particularly suitable to study properties of junction, interfaces, contacts, etc., wherein a small ac voltage is imposed across the device and the resulting ac current is measured over a pre-determined frequency range. The impedance spectra (a complex plane plot commonly known as *Nyquist Plot*) of the device is plotted in terms of real (Z') and imaginary (Z'') components of the impedance (Z^*), the values of which depend on the system parameters such as resistance (R), capacitance (C), angular frequency (ω) and a resistance (R_s) associated with the electrical contacts of the device and may be written as

$$Z^*(\omega) = Z' + Z'' = R_s + \frac{R}{1+(\omega RC)^2} - j\frac{\omega CR^2}{1+(\omega RC)^2} \quad (1)$$

In the recent past, IS has also been employed to measure the dynamic (ac) characteristics of solar cell [2,3] and induced junction structures [4]; and wherein cell parameters such as the dynamic resistance, transition capacitance, diode factor, effective minority carrier lifetime (τ_{eff}), series resistance, etc., were determined. The static (dc) characteristics of solar cells are routinely measured as dark and illuminated current–voltage (*I–V*) characteristics and spectral response (SR). From *I–V* curves the cell performance parameters such as open-circuit voltage (V_{oc}), short-circuit current density (J_{sc}), curve factor (CF), cell efficiency (η), diode factor and dark current are determined besides shunt and series resistances. The spectral response is a measure of device ability to collect charge carriers generated at different wavelengths of solar spectrum from which internal (Q_{int}) and external (Q_{ext}) quantum efficiencies, minority carrier diffusion length (L_b) in the base region, apparent dead layer thickness in the emitter and J_{sc} can be calculated. The use of IS in conjunction with *I–V* and SR measurements may provide comprehensive information about the quality of material, device performance, processing quality that may be vital for device characterisation, process development and designing of efficient device structures.

In this paper, we report IS, *I–V* and SR measurements on silicon solar cells from which static and dynamic device parameters were calculated. We have also tried to correlate IS, *I–V* and SR data.

2. Experimental

The experimental set-up for impedance measurement consists of a frequency response analyser (Solartron Model FRA, 1260A) and an electrochemical interface (Solartron Model ECI, 1287). FRA generates excitation signal (< 25 mV peak-to-peak to minimise

* Corresponding author. Tel.: +91 11 45608588; fax: +91 11 45609310.
E-mail address: pksingh@nplindia.org (P.K. Singh).

0927-0248/$ - see front matter © 2009 Elsevier B.V. All rights reserved.
doi:10.1016/j.solmat.2009.07.002

the distortion) of varying frequency (i.e., 10^{-2}–10^{6} Hz) that is applied to the device through ECI which acts as a sink and maintains the voltage across the device constant. The FRA measures both in phase and quadrature components and gives real and imaginary values of the cell impedance at different frequencies. The fitting of the data (in terms of impedance spectra in complex plane) was carried out using *Z*-plot software [5].

In the present study, an n^+–p–p^+ structure-based single-crystalline silicon solar cell ($2 \times 2\,cm^2$) has been used. The impedance (i) in dark, (ii) under different intensities of illumination and (iii) at different wavelengths keeping the intensity of heterogeneous light constant over a frequency range of 10^{-2}–10^{6} Hz was measured. All these measurements were done at zero bias condition. The intensity of xenon lamp was controlled by neutral density filters and for monochromatic radiations a set of narrow-band interference filters (FWHM = 10 nm) in 400–1050 nm range in the steps of 50 nm was used. *I–V* characteristics of the cell were measured under AM 1.5 (solar spectrum 100 mW/cm^2). The SR measurements were carried out using a set-up described in [6] wherein the same set of filters employed in IS measurements were used. All the measurements were performed at room temperature (25 °C).

3. Results and discussion

The dynamic equivalent circuit of a solar cell is derived from a static equivalent circuit by replacing the diode with the junction, transition and diffusion capacitances, and its dynamic resistance. The equivalent ac-circuit is shown in Fig. 1, wherein a single RC circuit consisting of a parallel resistor (R_p) and capacitor (C_p) exists and the impedance spectrum is, generally, a semicircle with its origin at (R_s+R_p/2, 0), where R_S is the series resistance of the device and the contribution from contacts. However, we presume that under illumination the entire light sensitive component in the structure provides a virtual *RC* (represented by R_1C_1) network parallel to the initial R_pC_p under work. The virtual R_1C_1 network appears due to illumination and can be attributed to the carrier generation in the device. Earlier Raniero et al. [7] have proposed a similar equivalent circuit for the p-i-n solar cells under illumination. To determine various parameters, the Nyquist plots were fitted into a parallel combination of single and double *RC* network in dark and under illumination conditions, respectively, using *Z*-plot software [5].

The measured current–voltage characteristic of the solar cell is shown in Fig. 2. The V_{oc}, J_{sc} and CF were found to be 588 mV, 28.55 mA/cm^2 and 0.61, respectively. The efficiency of the cell was 10.2% (AM = 1.5). Fig. 3 shows the measured spectral response and reflectivity of the solar cell as a function of λ. From SR and R_λ, the values of Q_{ext} and Q_{int} were calculated using the relations given in [6], which are plotted in the same figure. SR shows peaks at 850 nm from where the values of both Q_{ext} and Q_{int} decrease sharply with increase in λ.

The experimental values of the impedance spectra in dark and under heterogeneous light at different intensities of illumination (14, 43, 57, 71, 86 and 100 mW/cm^2) are shown in Fig. 4. The data obtained in dark were well fitted by Eq. (1), from which the values of R_s, R_p and C_p are deduced and the values are found to be 1.19 Ω, 2.29 KΩ and 229.1 nF, respectively. The light sensitive virtual R_1 and C_1 values are calculated at different intensities of light keeping R_p and C_p constant. The values of *R* and *C* are given in the Table 1 along with the estimated % error in their values (in brackets). It is found that the value of R_s, and; virtual R_1 and C_1 change with light intensity. The value of R_s is more under illumination compared with its value under dark condition.

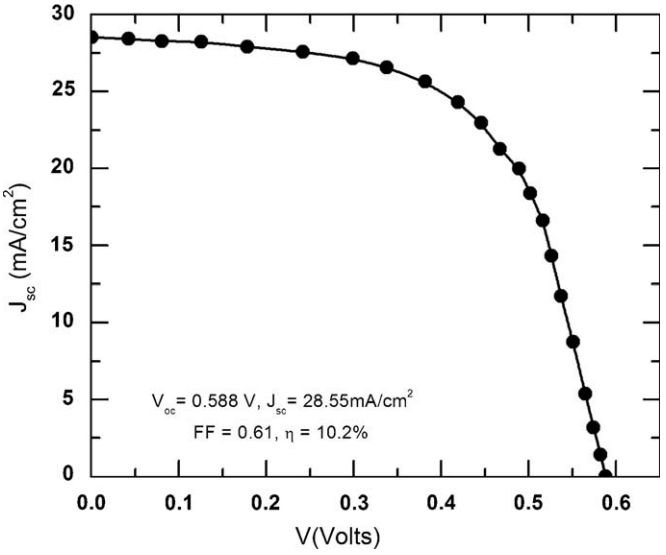

Fig. 2. *I–V* characteristics of the solar cell at 1 SUN under AM1.5.

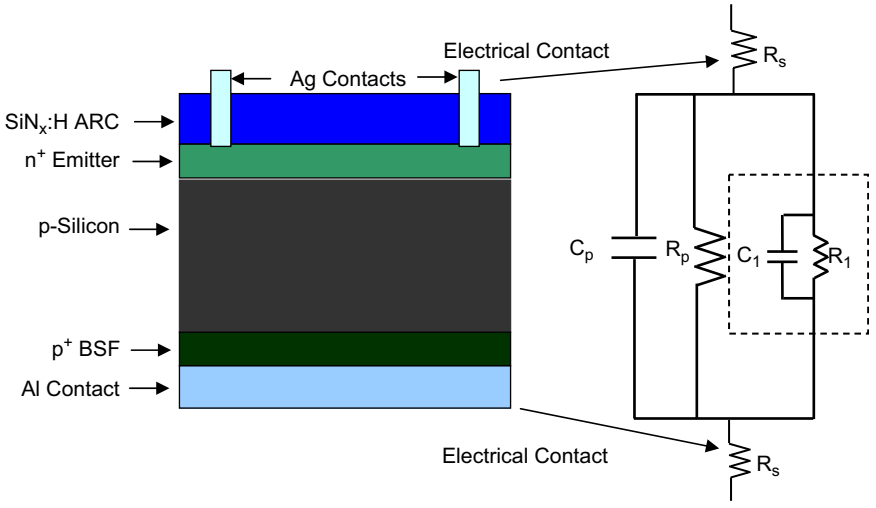

Fig. 1. Solar cell structure and its equivalent electrical circuit where R_s, R_p and C_p are the series resistance, bulk resistance and capacitance of the solar cell, respectively in the dark. R_1 and C_1 are the virtual resistance and capacitance respectively occur due to photo-carrier generation after illumination.

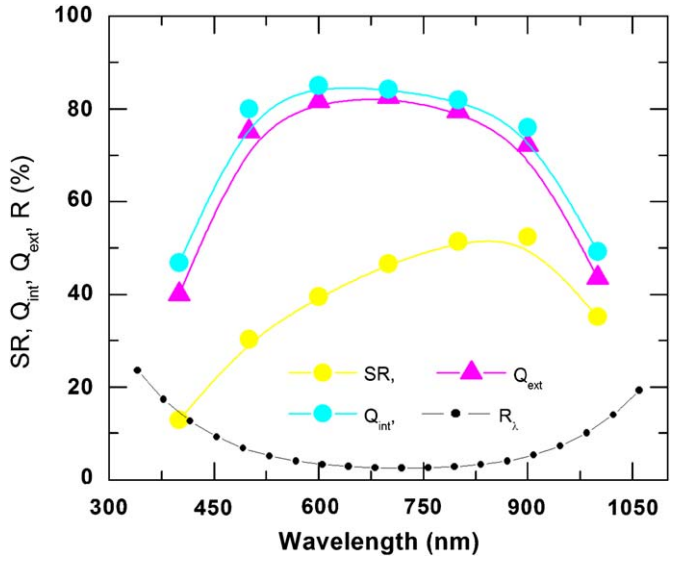

Fig. 3. (R_λ) Spectral response (SR) and internal (Q_{int}), external (Q_{ext}) efficiency and reflectivity of the solar cell.

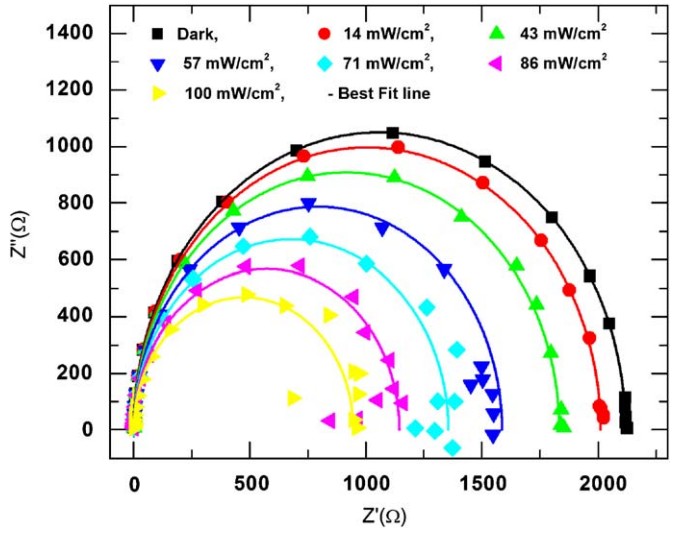

Fig. 4. Complex impedance spectra in dark and under different intensities (14, 43, 57, 71, 86, 100 mW/cm^2) of illumination where symbols represent experimental points and the lines Z-plot best fit curves, respectively.

Recently, similar behaviour of R_s under illumination was reported by El-Adawi and Al-Nuaim [8]. The value of R_s has also been determined using Araujo's area method [9] from the illuminated J–V characteristics curve at AM 1.5, which gave $R_s = 1.92\,\Omega$. This value is close to the value of this parameter obtained from the impedance spectra under illumination (100 mW/cm^2). On the other hand, R_1 and C_1 exhibit opposite trends where the value of the former as expected decreases and the latter increases with the intensity of light (P_{in}). The observed increase in capacitance under illumination can be explained by Moore's model [10,11], which states that under open-circuit conditions the value of capacitance does not change but under short-circuit condition an extra capacitance is added and the effective capacitance is defined as [11]

$$C_{eff} = C_d[1 + \delta] \quad (2)$$

where δ is proportional to the excess carrier concentration (Δn) that is directly related to P_{in} and hence to J_{sc}. Berry [12] has also

Table 1
Electrical contact resistance (R_s), bulk (R_p, C_p), and virtual (R_1, C_1) for different intensities obtained from the best fit of the complex plane impedance data using Z-plot software.

P_{in} (mW/cm^2)	R_s (Ω)	R_p (kΩ)	C_p (nF)	R_1 (kΩ)	C_1 (nF)
Dark	1.19 [5.96]	2.12 [0.15]	229.1 [0.37]	–	–
14	2.33 [5.17]	2.12 [0.16]	229.1 [0.61]	43.0 [0.12]	0.10 [1.43]
43	2.23 [12.43]	2.12 [0.14]	229.1 [0.55]	14.49[0.14]	0.10 [1.81]
57	2.20 [10.37]	2.12 [0.14]	229.1 [0.30]	5.67[0.18]	0.10 [1.77]
71	1.59 [13.49]	2.12 [0.18]	229.1 [0.33]	3.91[0.13]	1.60 [1.06]
86	1.55 [12.07]	2.12 [0.15]	229.1 [0.26]	2.48[0.14]	5.62 [1.15]
100	1.97 [13.90]	2.12 [0.19]	229.1 [0.51]	1.68[0.11]	6.02 [1.51]

The values given in the brackets are estimated % error in the respective parameter values.

Table 2
Electrical contact resistance (R_s), bulk (R_p, C_p), and virtual (R_1, C_1) for different wavelength λ obtained from the best fit of the complex plane impedance data using Z-plot software.

λ (nm)	R_s (Ω)	R_p (kΩ)	C_p (nF)	R_1 (kΩ)	C_1 (nF)
Dark	1.19 [5.96]	2.12 [0.15]	229.1 [0.37]	–	–
400	1.17 [10.09]	2.12 [0.15]	229.1 [0.45]	10.97 [0.12]	1.03 [1.14]
500	1.52 [12.51]	2.12 [0.16]	229.1 [0.49]	10.35 [0.13]	1.30 [1.36]
600	1.07 [12.63]	2.12 [0.15]	229.1 [0.51]	9.65 [0.19]	1.69 [0.74]
700	0.89 [10.40]	2.12 [0.14]	229.1 [0.48]	9.14 [0.14]	0.93 [1.03]
800	1.13 [11.31]	2.12 [0.13]	229.1 [0.37]	7.96 [0.16]	0.49 [0.85]
850	**0.62 [14.79]**	**2.12 [0.13]**	**229.1 [0.34]**	**6.50 [0.19]**	**0.77 [1.61]**
950	0.87 [12.95]	2.12 [0.14]	229.1 [0.36]	7.94 [0.18]	0.14 [0.89]
1000	0.69 [12.22]	2.12 [0.16]	229.1 [0.56]	8.88 [0.16]	1.04 [0.61]
1050	0.70 [10.99]	2.12 [0.18]	229.1 [0.58]	9.30 [0.17]	1.02 [0.57]

The values given in the brackets are estimated % error in the respective parameter values.

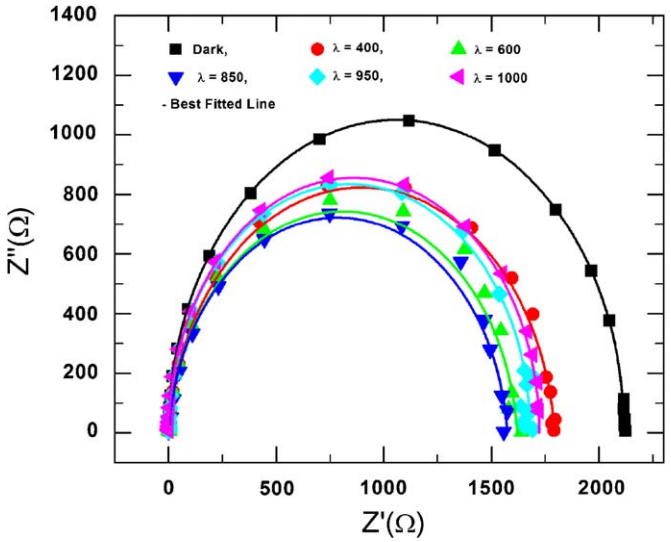

Fig. 5. Complex impedance spectra in dark and at different (400, 600, 850, 1000 nm) wavelength of irradiation. The symbols represent experimental points and the lines gives best fit curves from Z-plot software.

reported a similar behaviour in C_1 under illumination. Moore also predicted C_d dependence on spectral distribution (λ). Therefore, the observed change in the C_1 with P_{in} and λ (shown in Tables 1 and 2 respectively) is not unexpected. However, the difference in C_1 was not significant at low intensities (<50 mW/cm^2).

Table 2 shows the values obtained from impedance spectra at different wavelengths (400–1050 nm) by keeping the intensity of heterogeneous light constant (<50 mW/cm^2) over the frequency range of 10^{-2}–10^6 Hz. In Fig. 5 impedance spectra only for

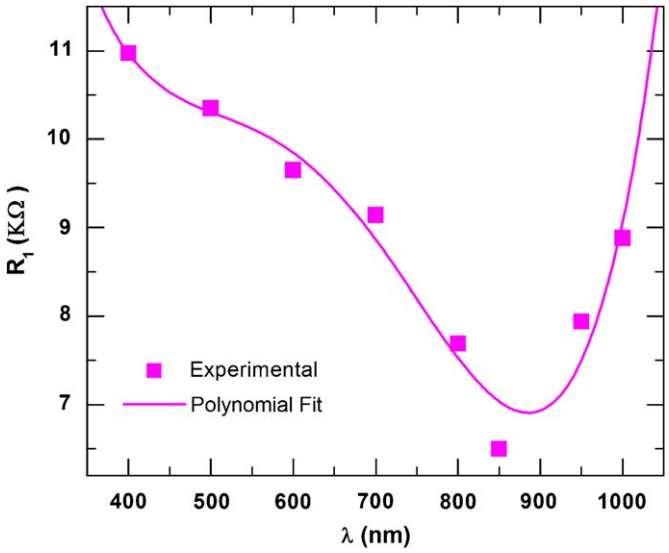

Fig. 6. Virtual Resistance (R_1) vs. wavelength (λ). The data has been obtained from the complex plane impedance data using *Z*-plot software.

wavelengths of 400, 600, 850, 950 and 1000 nm are presented for the sake of clarity. The data suggest that the values for R_s have different values which can be correlated to the absorption depth at different wavelengths of light. On the other hand, the values of virtual R_1 and C_1 depend on the wavelengths as well as on the number of carriers generated (i.e., δ dependence on Δn) in the device. It is to be noted that the values of R_p and C_p (2.12 KΩ and 229 nF, respectively) obtained from the impedance data in dark are assumed to be the same for calculation of R_1 and C_1 for all wavelengths, therefore, the virtual R_1C_1 circuit manifests the effect of illumination. It is found that the impedance curve starts shrinking from low λ (e.g., 400 nm) up to 850 nm from where it begins to expand and are smaller compared with their dark values at all wavelengths. This observation is further supported by the SR or QE data (Fig. 3) as the minimum value of R_1 (Fig. 6) corresponds to the maximum value of SR at 850 nm. It is to be remarked here that SR and R_1 data are complementary to each other in the 400–1050 nm range.

4. Conclusions

The dynamic and static characteristics of an n+–p–p+ structure-based single-crystalline silicon solar cell were measured by impedance spectroscopy (IS), *I–V* and spectral response (SR). The IS measurements were carried out in dark and at different intensities of illumination (0–100 mW/cm^2) and at different wavelengths (400–1050 nm). The IS data were analysed using frequency response analyser software from which various circuit parameters were determined. The values of virtual R_1 and C_1 depend on the illumination wavelengths. This observation can be correlated with SR or QE data as the minimum and maximum values of R_1 or C_1 correspond to the maximum and minimum values of SR, respectively.

Acknowledgements

The authors thank the Director, NPL for the permission to publish this work. One of the authors, SK, acknowledges financial support by the Ministry of New & Renewable Energy, Government of India in the form of research fellowship..

References

[1] J.R. Mac Donald, W.B. Johnson, Impedance Spectroscopy, Wiley, New York, 1987.
[2] R. Anil Kumar, M.S. Suresh, J. Nagaraju, Facility to measure solar cell AC parameters using an impedance spectroscopy technique, Review of Scientific Instruments 72 (8) (2001) 3422–3426.
[3] G. Friesen, M.E. Ozsar, E.D. Dunlop, Impedance model for CdTe solar cells exhibiting constant phase element behaviour, Thin Solid Films 361–362 (2000) 303–308.
[4] S. Kumar, R. Srivastava, G.S. Chilana, P.K. Singh, Application of an impedance spectroscopy technique to study silicon solar cells and induced n+–p–p+ junction structures, Journal of Optoelectronics and Advanced Materials 9 (2) (2007) 371–374.
[5] Z Plot Software Application, version 2, Scribner Associates Inc., Southen Pines, NC, USA.
[6] P.K. Singh, R. Kumar, P.N. Vinod, B.C. Chakravarty, S.N. Singh, Effect of spatial variation of incident radiation on spectral response of a large area silicon solar cell and the cell parameters determined from it, Solar Energy Material and Solar Cells 80 (2003) 21–31.
[7] L. Raniero, E. Fortunato, I. Ferreira, R. Martins, Study of nanostructured/amorphous silicon solar cell by impedance spectroscopy technique, Journal of Non-Crystalline Solids 352 (2006) 1880–1883.
[8] M.K. El-Adawi, I.A. Al-Nuaim, A method to determine the solar cell series resistance from a single *I–V*. Characteristic curve considering its shunt resistance-new approach, Vacuum 64 (2002) 33–36.
[9] G.L. Araujo, E. Sancez, A new method for experimental determination of the series resistance of a solar cell, IEEE Transactions on Electron Devices ED-29 (10) (1982) 1511–1513.
[10] A.R. Moore, Solar cell capacitance, RCA Review 36 (1975) 551–565.
[11] A.R. Moore, Short-circuit capacitance of illuminated solar cells, Applied Physics Letters 27 (1) (1975) 26–29.
[12] W.B. Berry, Photovoltaic short-circuit minority carrier injection, Applied Physics Letters 25 (4) (1974) 195–196.